Ion energy distributions and densities in the plume of Enceladus

Shotaro Sakai[1]

Collaborators

Thomas E. Cravens[1], Nojan Omidi[2], Mark E. Perry[3], J. Hunter Waite Jr.[4]

1: *Department of Physics and Astronomy, University of Kansas*

2: *Solana Scientific Inc.*

3: *The Johns Hopkins University Applied Physics Laboratory*

4: *Southwest Research Institute*

Outline

- Enceladus, Saturn’s inner magnetosphere and E ring
- Enceladus plume observations
  - Cassini INMS and CAPS
- Model description
  - Equation, chemical reactions, model settings…
  - Some cases of electric and magnetic field
- Results & Discussions
  - Model comparisons with CAPS, INMS and LP
- Summary

Enceladus

- Enceladus (~3.95 R_S)
  - Equatorial radius: 247 km
  - Orbital radius: 238.02 x 10^3 km
    - ~3.95 R_S
  - Mass: 7.0 x 10^{19} kg
  - Atmosphere: (Thin) Water vapor

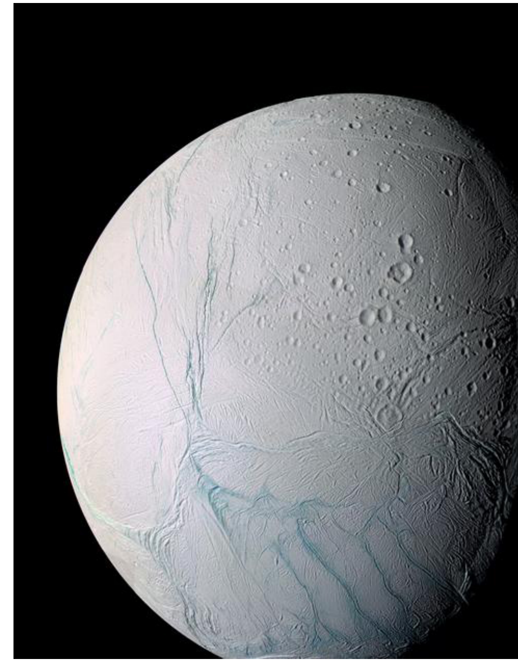

Enceladus [*NASA*]

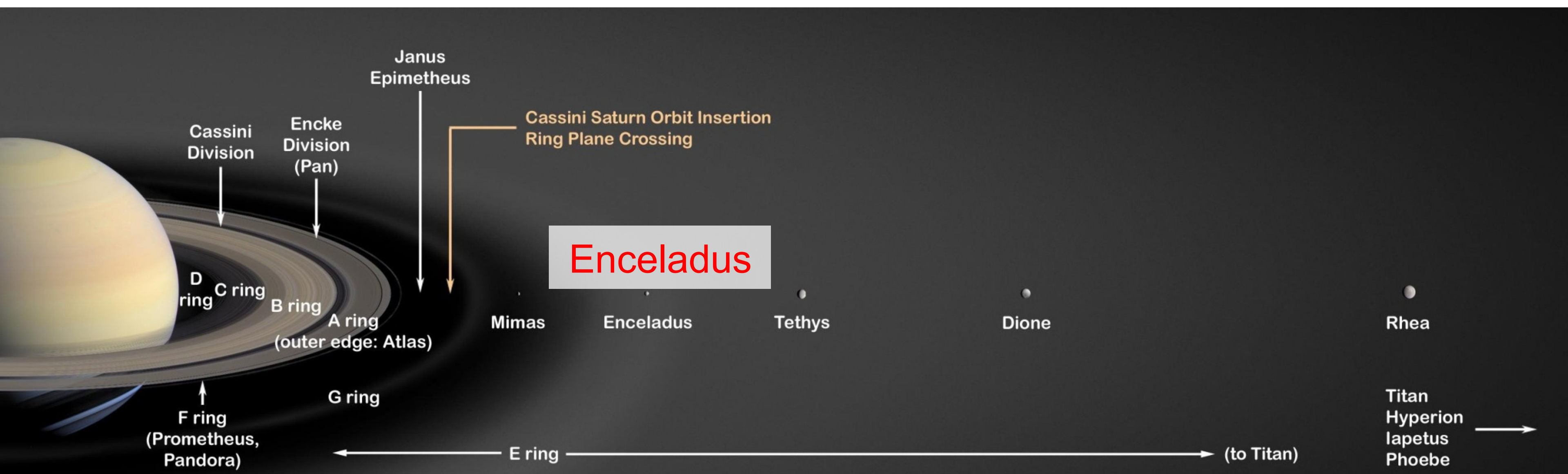

Enceladus plume & E ring

- Enceladus plume (~3.95 R_S)
  - Water gas
- E ring
  - 3 – 8 R_S (overlapping with inner magnetosphere)
  - Water group ion
  - Dust
  - Source: Mainly Enceladus plume

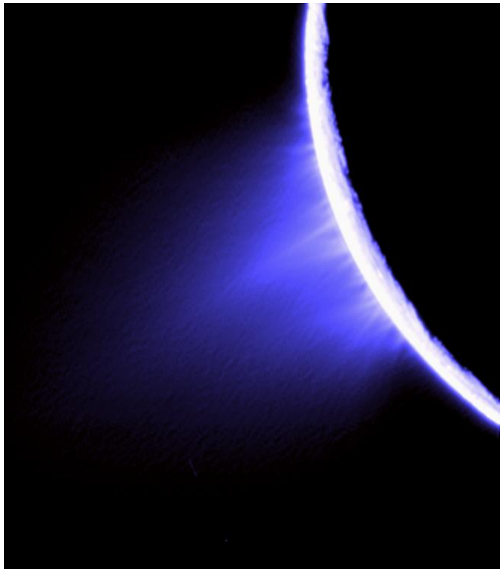

Enceladus & E ring [*NASA/JPL*]

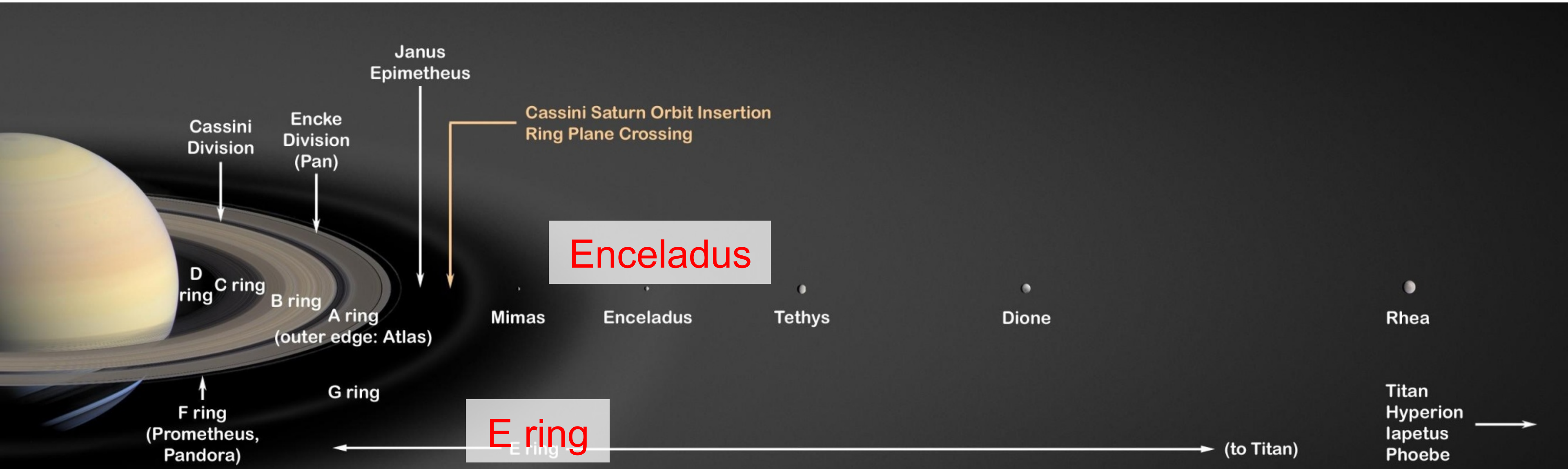

Cassini

- Outline
  - Launch date: Oct. 15,1997
  - Development & Operation: NASA, ESA
  - Orbit Insertion: Jul. 1, 2004
  - Now Operating!
    - EOM: Sep. 15(?), 2017
- Instruments (3 major)
  - Optical remote sensing
  - Electric-magnetic field, particles and wave observation
  - Microwave remote sensing

Cassini [*Gurnett et al.*, 2004]

INMS & CAPS

- Ion and Neutral Spectrometer (INMS)
  - Can measure the mass number of ions and neutrals (1 < amu < 99)
  - Two sources
    - Closed source: ex. N_2, CH_4
      - Species not to react with the antechamber surface
    - Open source: Radicals and ions

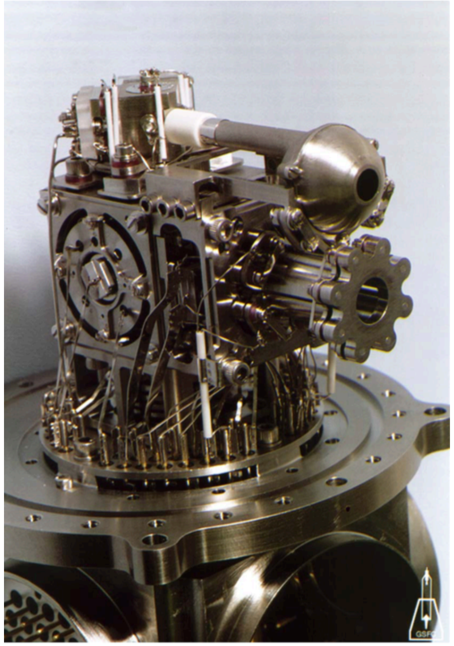

INMS [*Waite et al.*, 2004]

- Cassini Plasma Spectrometer (CAPS)
  - Electron spectrometer (ELS)
    - Electron energy distribution
  - Ion mass spectrometer (IMS)
    - Ion energy (and mass) distribution
  - Ion beam spectrometer (IBS)

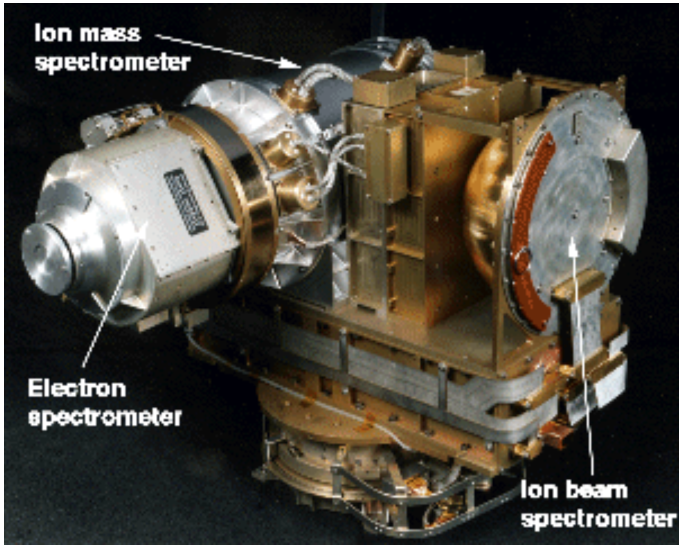

CAPS [*UCL*]

Enceladus flybys

- Enceladus plume encounter
  - Cassini had 22 Enceladus orbits.
  - E03 and E07 orbits are the focus of this presentation.

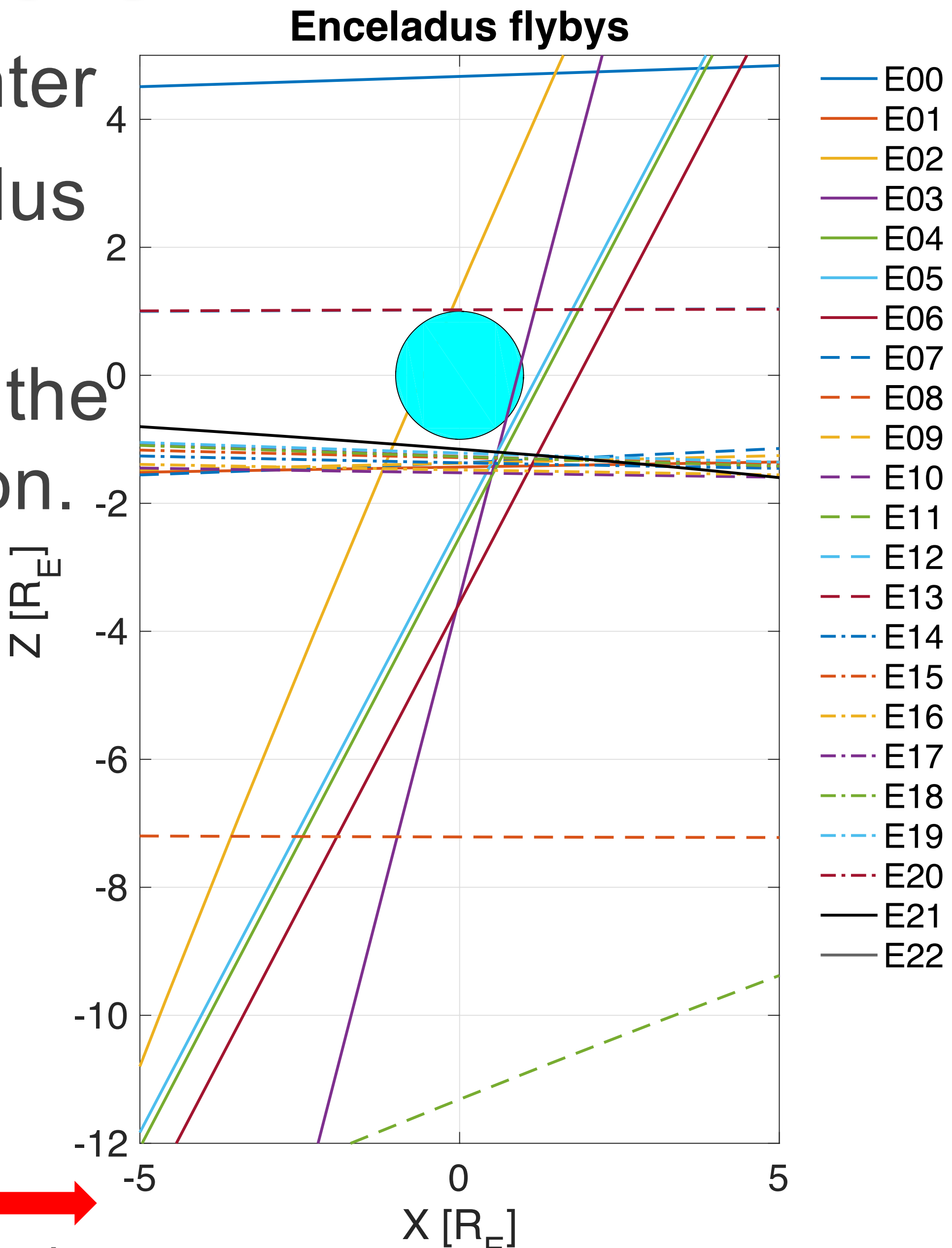

Co-rotation direction

Enceladus flybys

- Enceladus plume encounter
  - Cassini had 22 Enceladus orbits.
  - E03 and E07 orbits are the focus of this presentation.

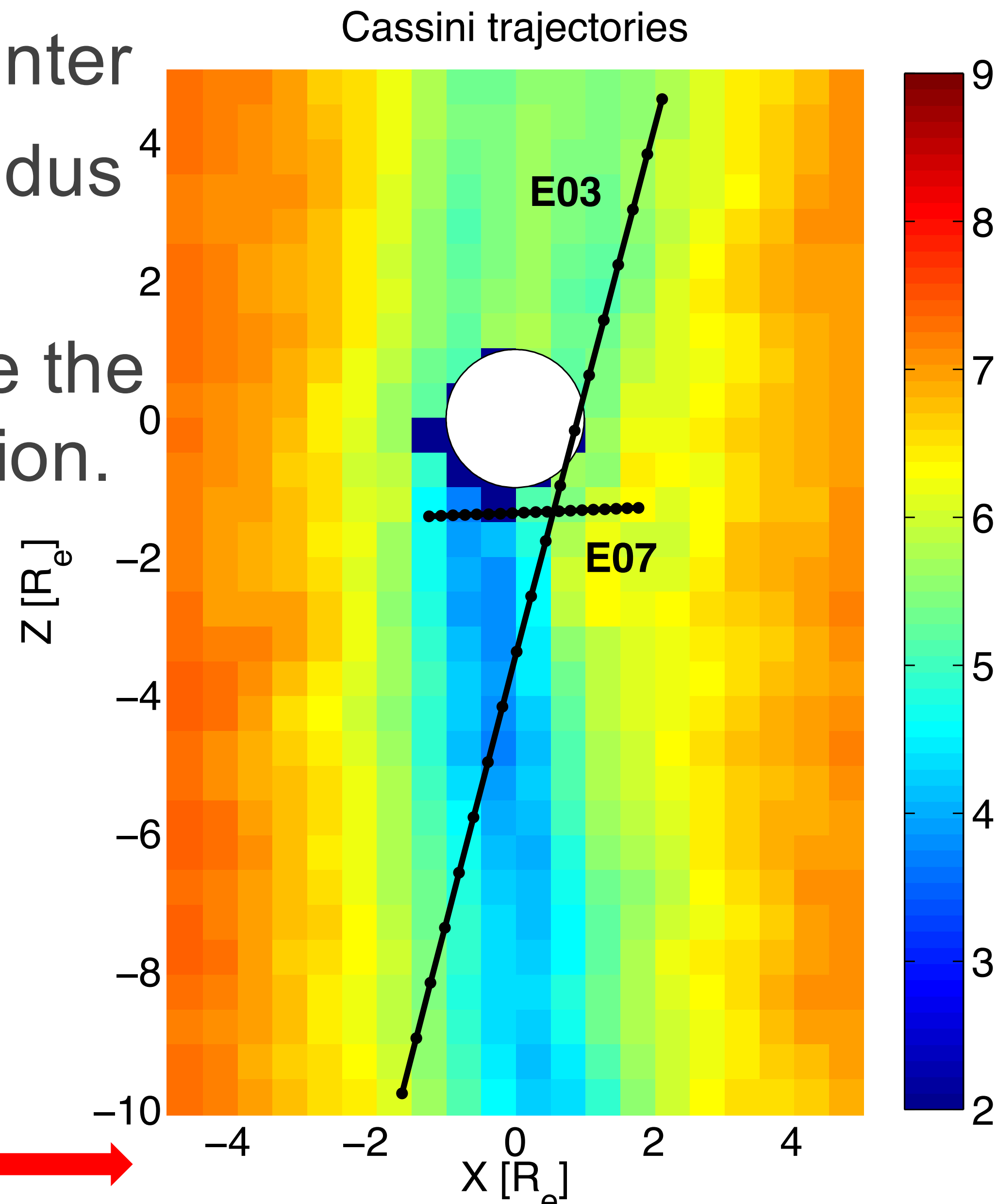

[*Sakai et al.*, 2016]

Ion species in the plume

- INMS observations in the plume for E03 orbit
  - H_3O^+ is dominant. $H_2O^+ + H_2O \rightarrow H_3O^+ + OH$

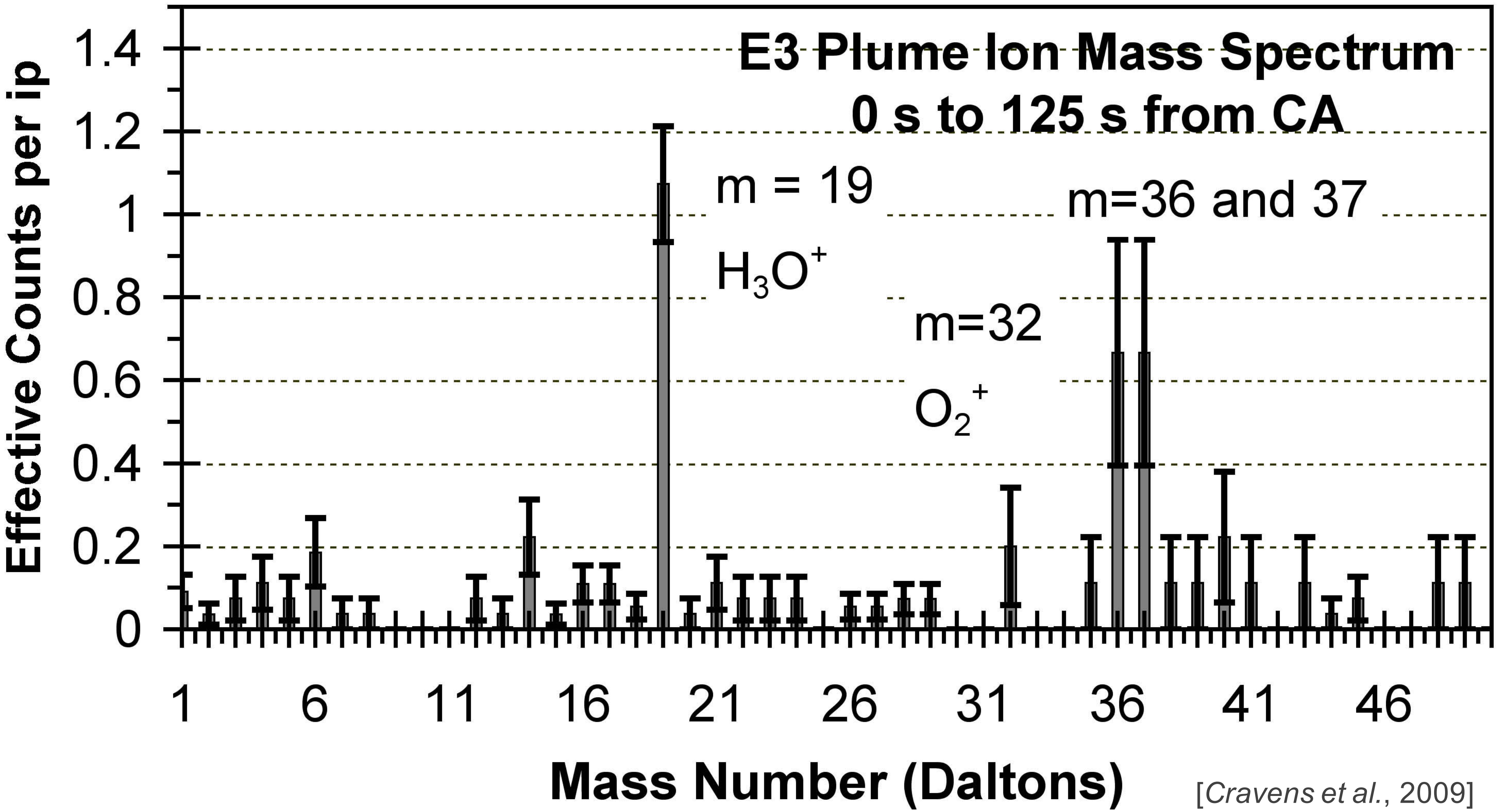

[*Cravens et al.*, 2009]

INMS (H_2O^+ & H_3O^+) for E03 & E07

- INMS counts
  - H_3O^+ is dominant.
  - Max.: ~10

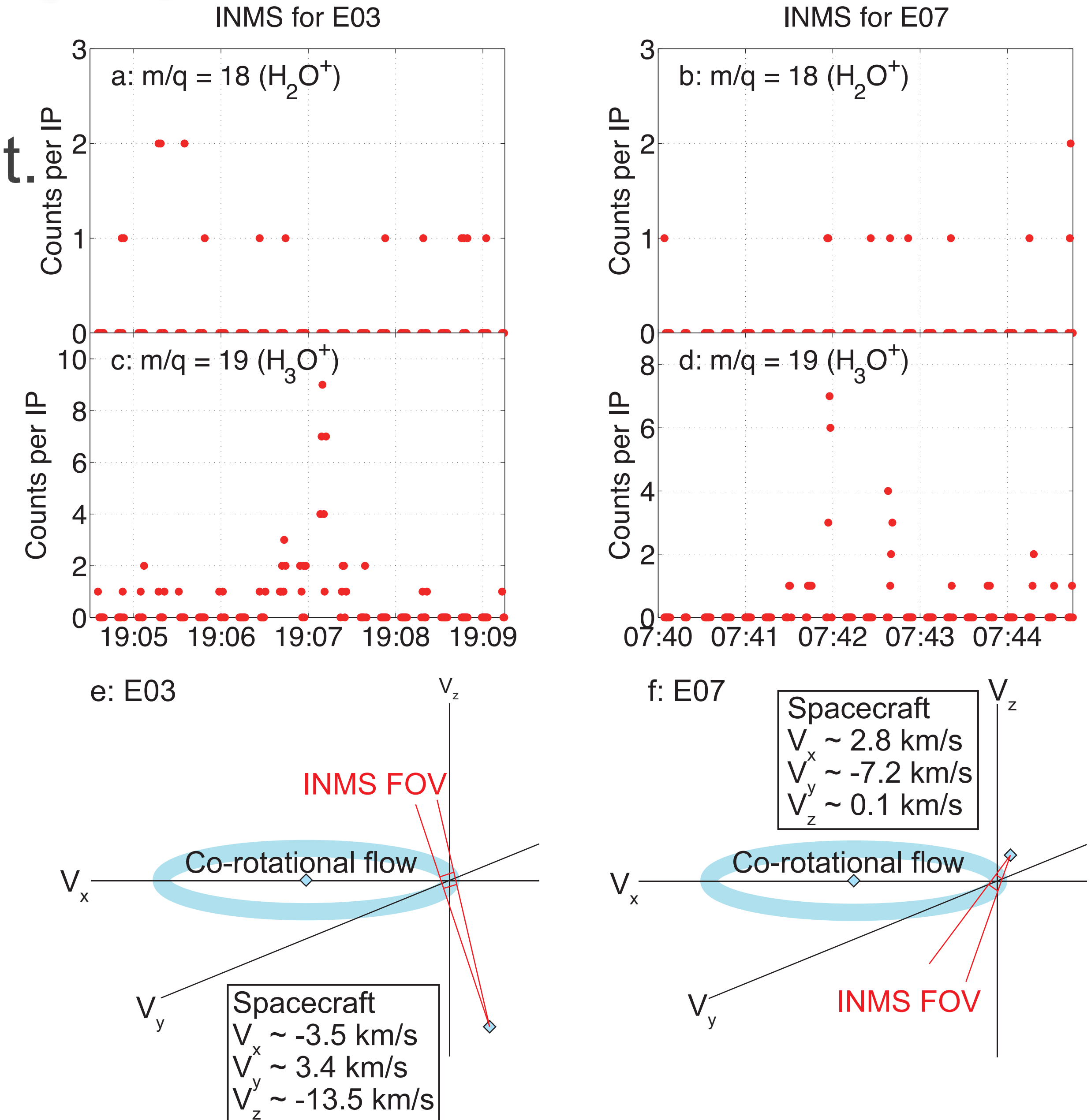

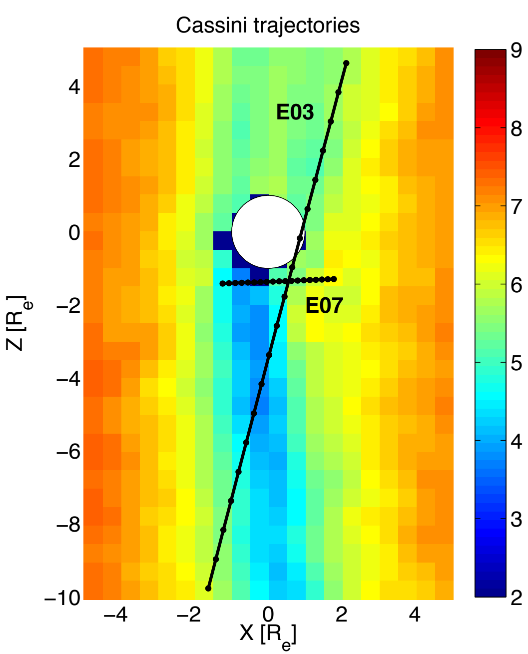

[*Sakai et al.*, 2016]

CAPS/IMS for E03 & E07

- CAPS energy spectrum
  - Low energy plasma
    - ~19:07 for E03; ~07:42 for E07

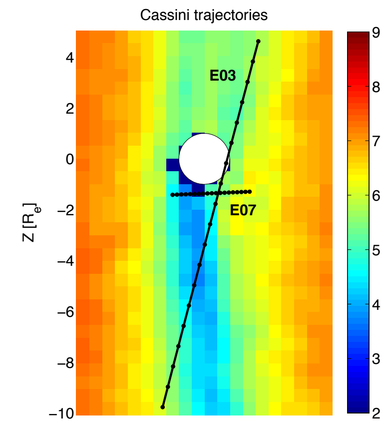

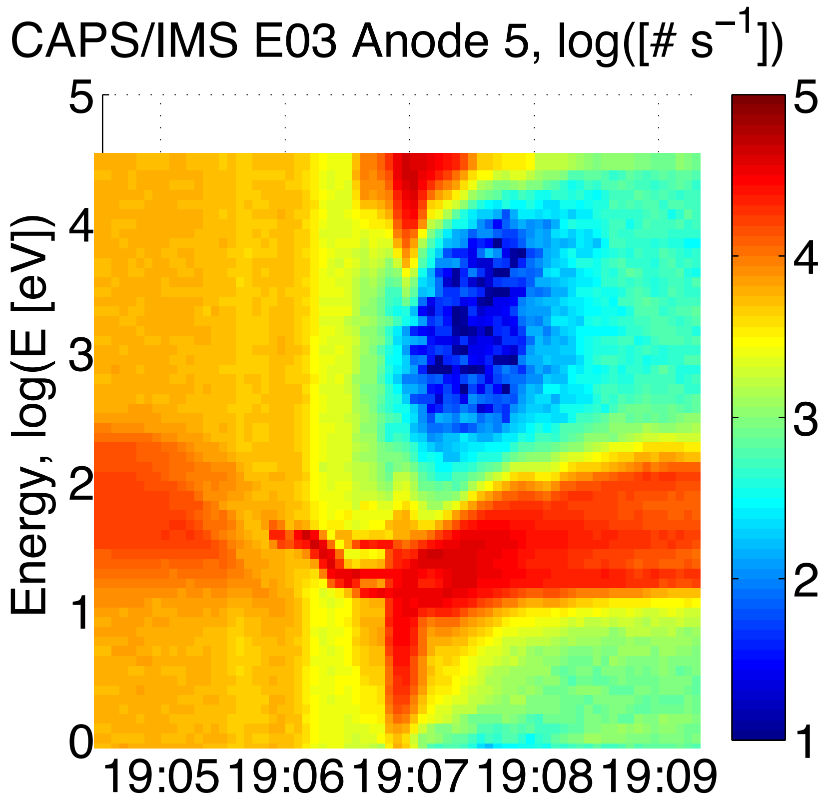

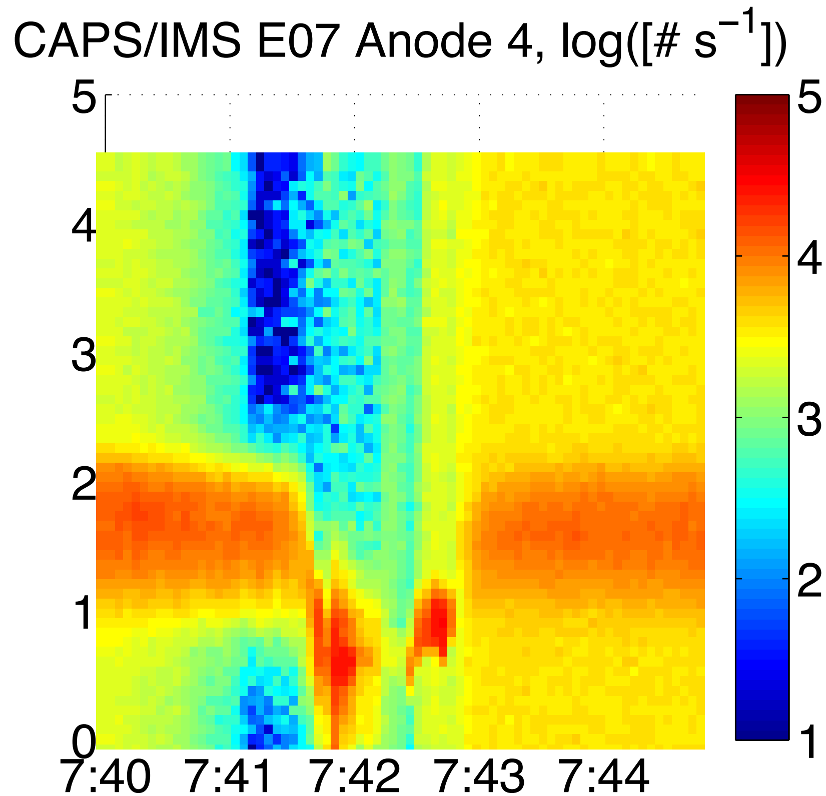

[*Sakai et al.*, 2016]

Motivation & Method

- Investigation of the ion environment in Enceladus plume
  - Where do low energy ions come from?
  - What are the physical processes need to explain INMS (and CAPS) data?
    - Electric field or Magnetic field?

- Method
  - Test-particle simulation of water group ions

Test particle simulation

- Equation of motion

$$m_i \frac{d\mathbf{v}_i}{dt} = q(\mathbf{E} + \mathbf{v}_i \times \mathbf{B})$$

- Enceladus coordinate system

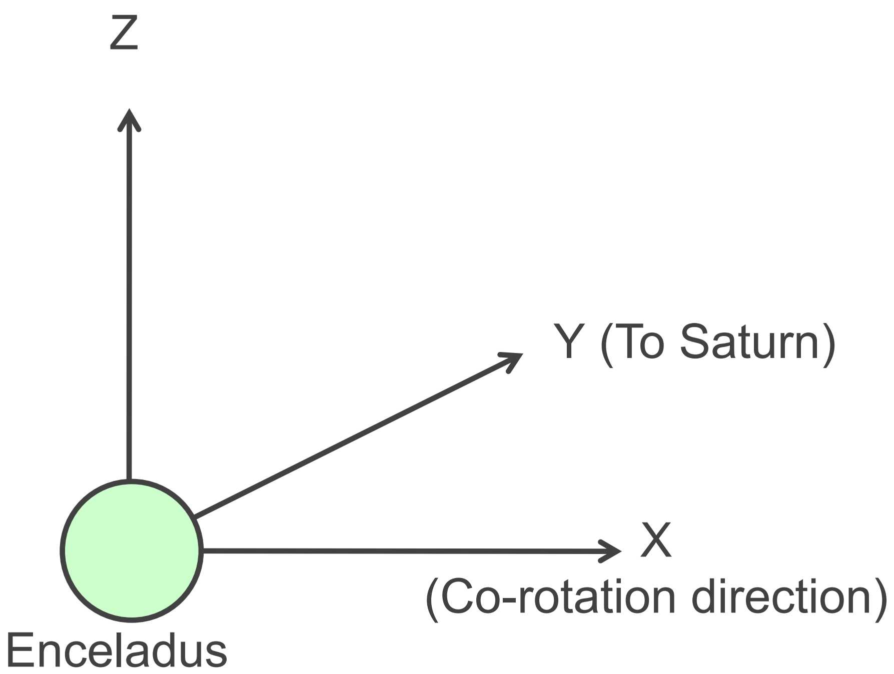

Models

- Where do ions in the plume come from?
  1. Charge exchange between background ions and neutral plume
     - Charge eXchange front model (CX model)
  2. Photoionization in the plume
     - Photoionization Plume model (PP model)

Models

- Where do ions in the plume come from?
  1. Charge exchange between background ions and neutral plume
     - Charge eXchange front model (CX model)
  2. Photoionization in the plume
     - Photoionization Plume model (PP model)

Test particle simulation

- Charge eXchange Front Model (CX)
  - Interaction of the background ion with the plume gas
  - Particle generator: H_2O^+ at X = -5 R_E
  - Initial V based on the bulk speed: V_z = 0
    - Disk input (particle number of 5 millions)
      - Ion velocity is smaller than the co-rotation velocity in the inner magnetosphere [*Holmberg et al.*, 2012, *Sakai et al.*, 2013].

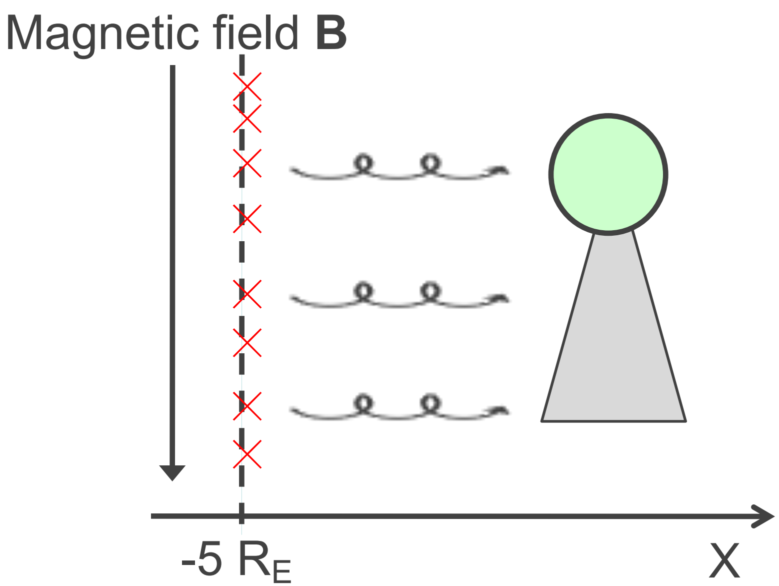

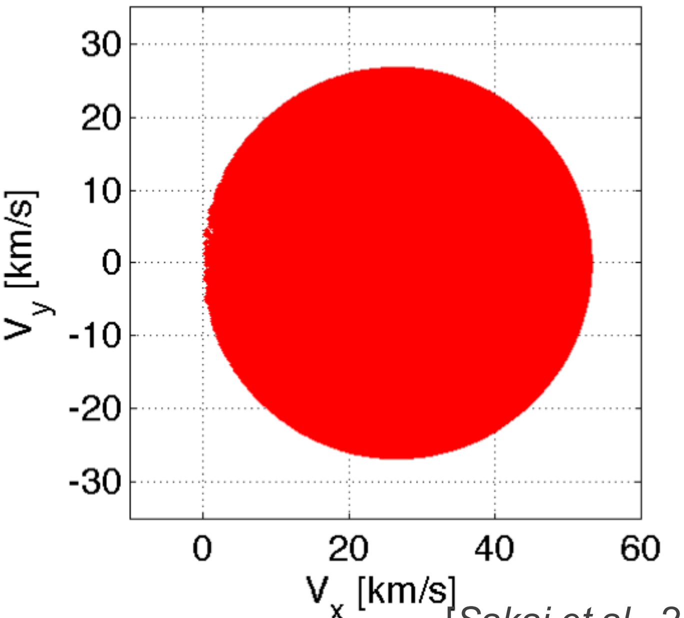

[*Sakai et al.*, 2016]

Simulation settings

- Area of simulation
  - $-5\ R_E < X < 5\ R_E$; $-5\ R_E < Y < 5\ R_E$; $-10\ R_E < Z < 5\ R_E$
    - Move to next particle when a particle is out of this area.
- Plume neutral density (H_2O gas)
  - Based on *Saur et al.* [2008]

$$n_{plume} = n_0 \left(\frac{R_E}{r} \right)^2 \exp\left[-\left(\frac{\Theta}{H_\Theta} \right)^2 - \frac{r - R_E}{H_d} \right]$$

  - $n_0 = 2.5 \times 10^9\ cm^{-3}$, $H_\Theta = 12$ deg., $H_d = 948$ km [*Fleshman et al.*, 2010]

Reactions with the plume

- H_2O^+ & H_3O^+
- Charge exchange & Chemical reactions

$$H_2O^+ + H_2O \rightarrow H_2O + H_2O^+$$
$$H_2O^+ + H_2O \rightarrow OH + H_3O^+$$

  - Monte Carlo method for reactions
- H_3O^+-H_3O^+ collisions
  - Elastic scattering
  - The cross section is based on a H^+-He cross section [*Krstic and Schultz*, 1999], but we scale it by a factor of 10.

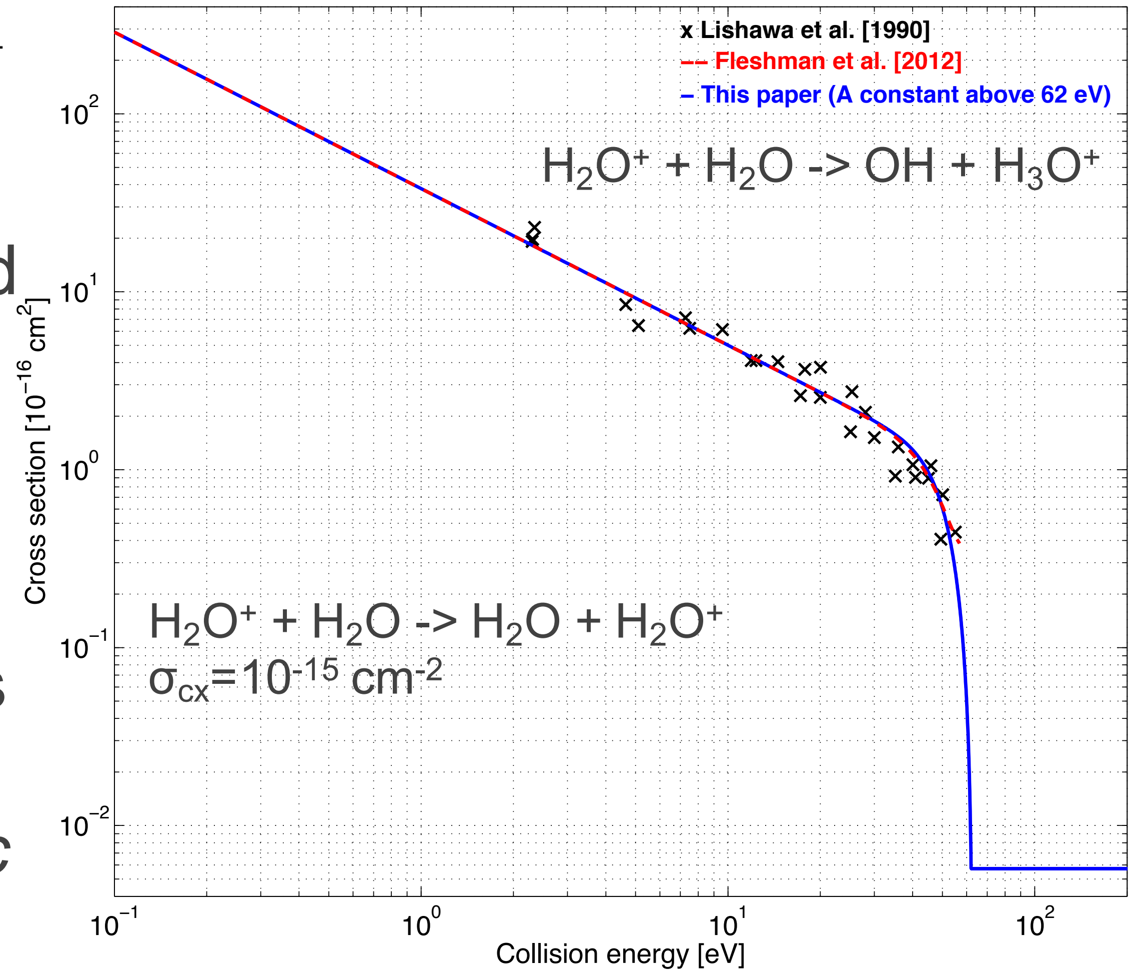

[*Sakai et al.*, 2016]

Chemical reactions

- H_2O^+ -> H_3O^+ [*Lishawa et al.*, 1990]
  - Proton transfer channel

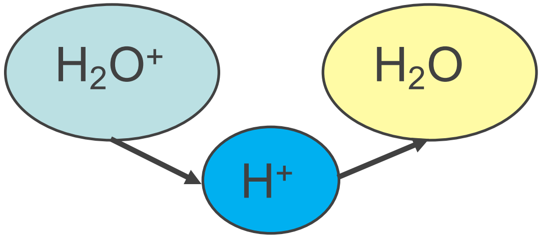

  - Atom pickup channel

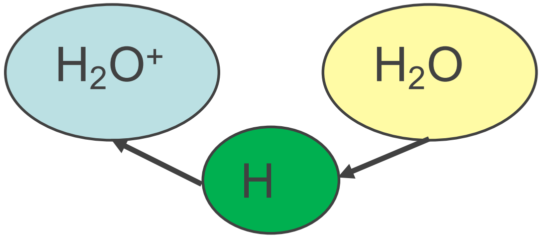

  - $\sigma_{pt} > \sigma_{api}$, so the proton transfer channel is adopted.
    - One order of magnitude higher

Chemical reactions

- H_2O^+ -> H_3O^+ [*Lishawa et al.*, 1990]
  - Proton transfer channel

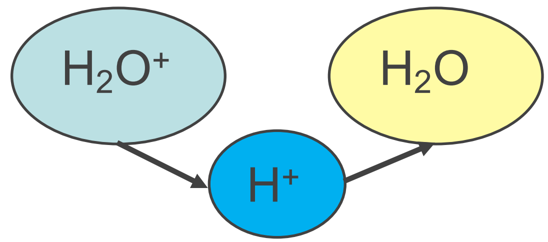

  - Atom pickup channel

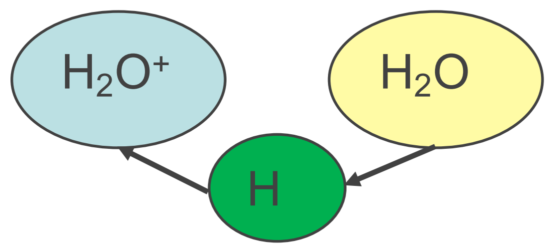

  - $\sigma_{pt} > \sigma_{api}$, so the proton transfer channel is adopted.
    - One order of magnitude higher

BE fields for E03 & E07

- Magnetic and electric fields used in this simulation

- Based on *Omidi et al.* [2012]
- 3 cases for E in the plume
  - 1) Omidi's field
    - No changes
  - 2) Reduced E_y
    - 25% of Omidi's E_y
  - 3) Reduced E_y & E_z
    - 25% of Omidi's E_y
    - E_z = -10 μV/m

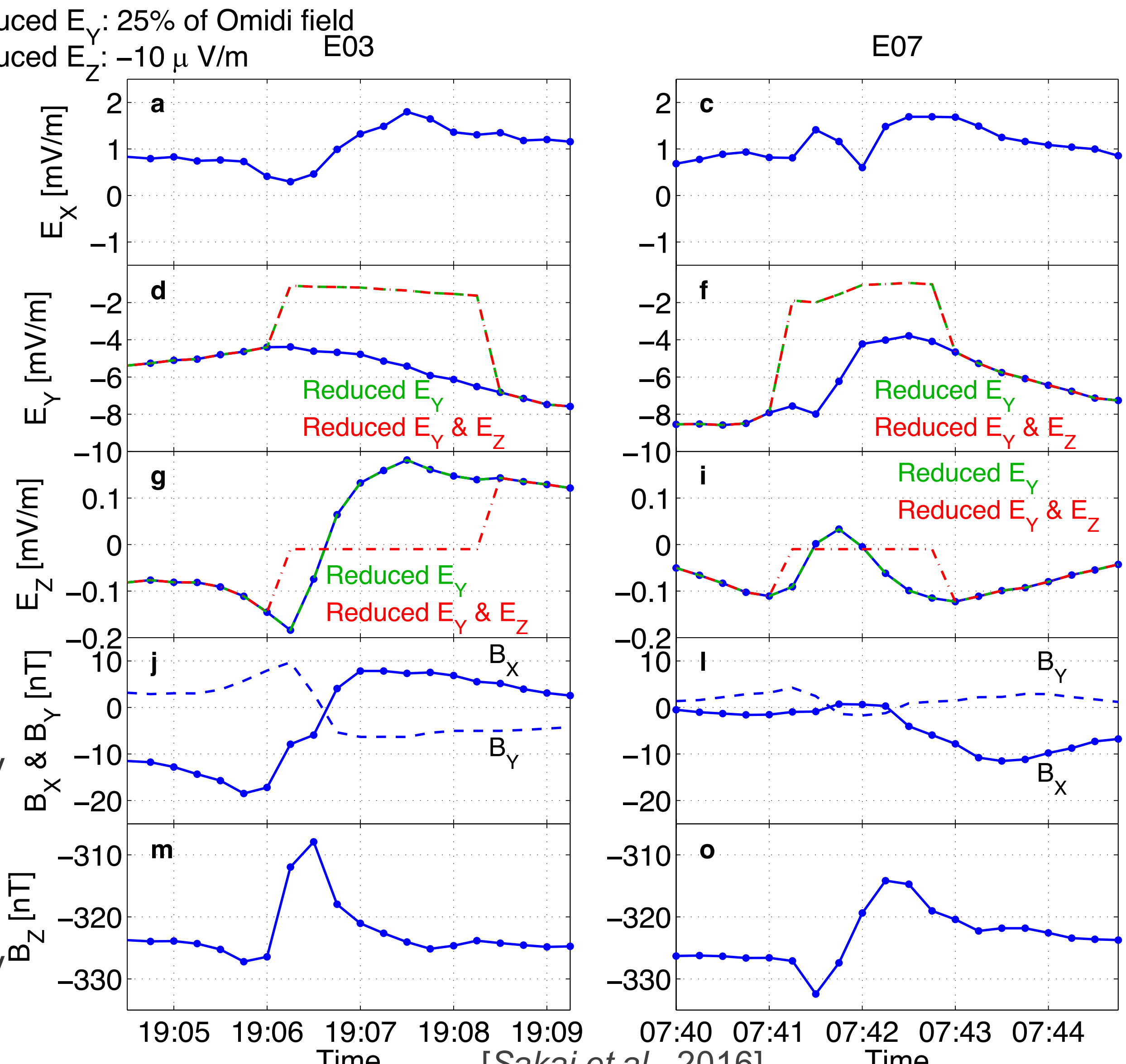

[*Sakai et al.*, 2016]

Before showing results

- What are outputs of this simulation?
  - The number of particles into each bin
  - Example of bin

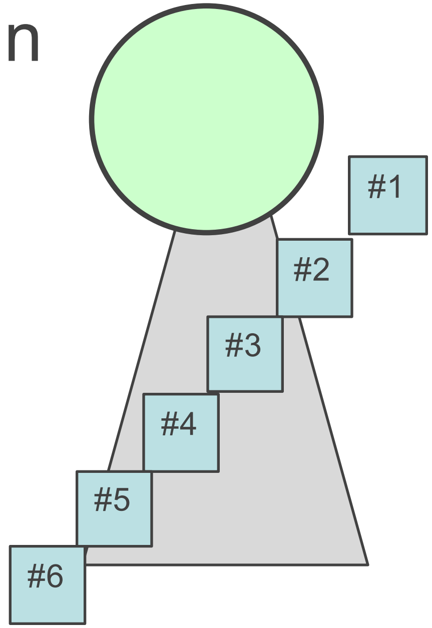

  - Convert this number to flux, total count for INMS comparison and density every bin.

Results

Results: Flux for E03 & E07

- Energy vs. Flux distribution (Cassini reference frame)
- E_z is important for obtaining the low energy ion.
- Ions are moving to –Z direction.
- E_z can be generated by dust [e.g., *Farrell et al.*, 2010] or pressure gradient of plasma in Z direction.
- Note that the units of models are different from CAPS.

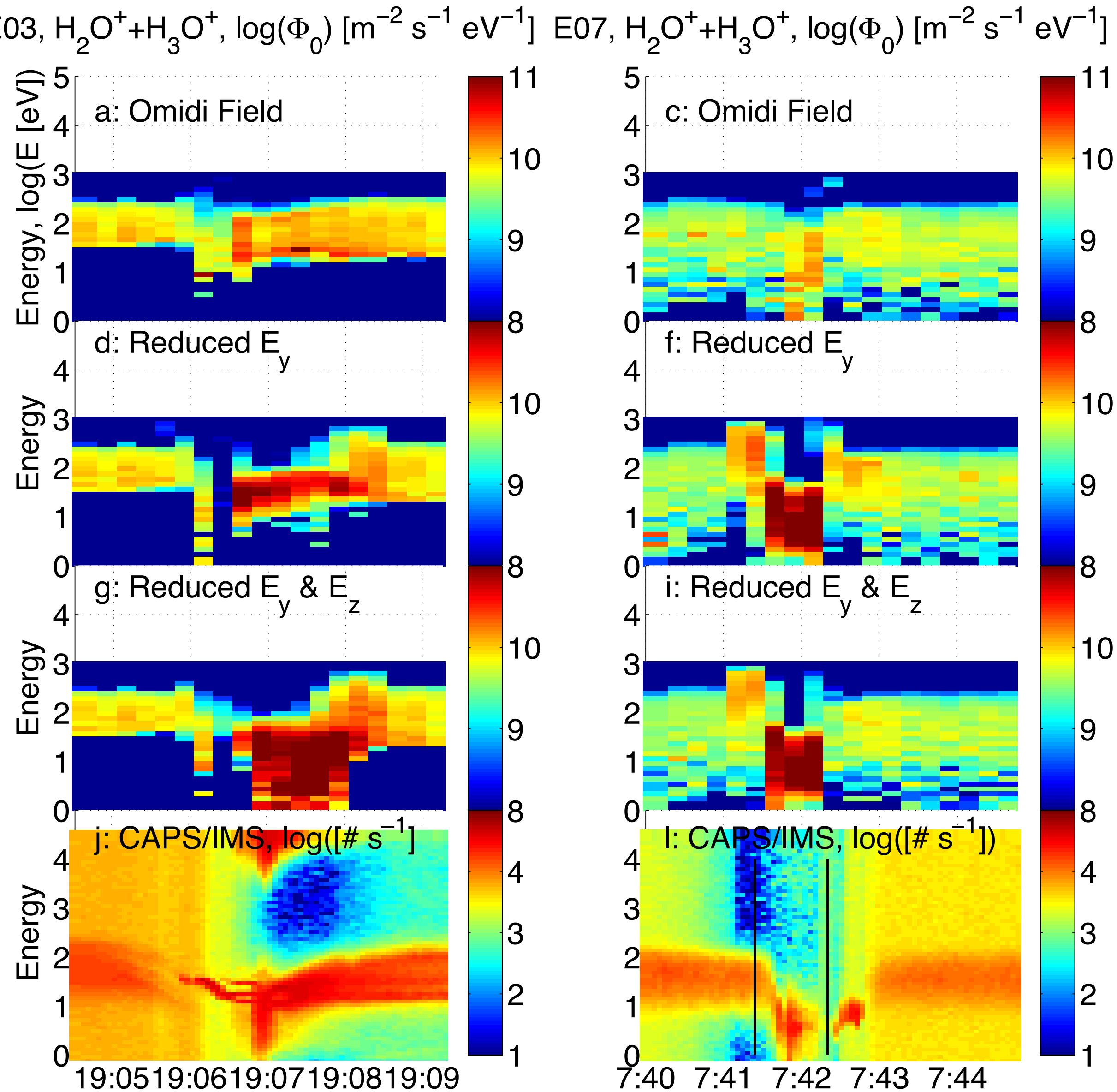

[*Sakai et al.*, 2016]

Ion counts: Comparison with INMS

- Calculated ion counts: INMS: ≈10, Model: 100-1000

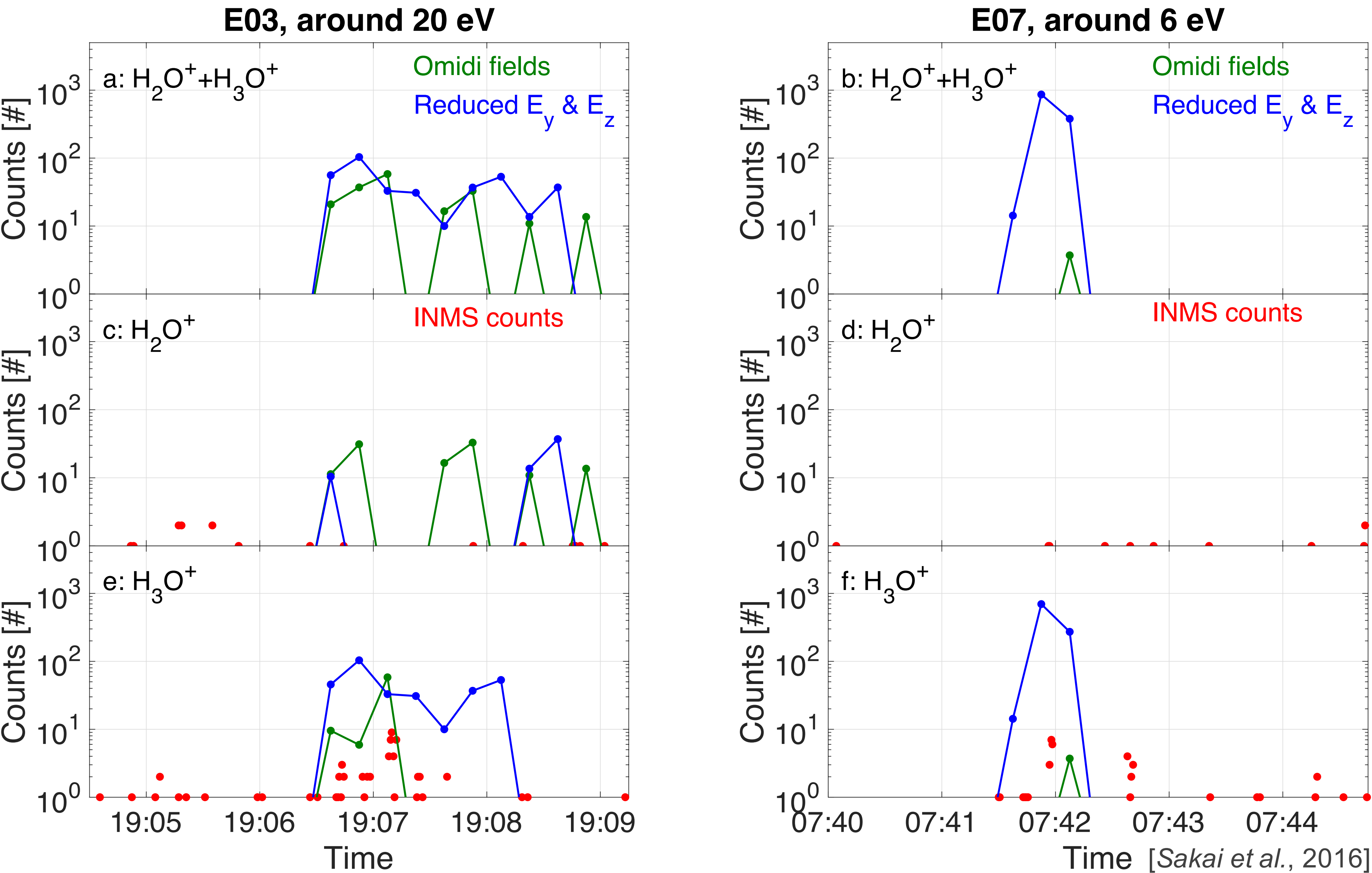

[*Sakai et al.*, 2016]

Models

- Where do ions in the plume come from?
  1. Charge exchange between background ions and neutral plume
     - Charge eXchange front model (CX model)
  2. Photoionization in the plume
     - Photoionization Plume model (PP model)

Models

- Where do ions in the plume come from?
  1. Charge exchange between background ions and neutral plume
     - Charge eXchange front model (CX model)
  2. Photoionization in the plume
     - Photoionization Plume model (PP model)

Photoionization

- Photoionization Plume Model (PP)
  - See ions generated by photoionization
  - Particle generator: H_2O^+ in the plume
  - Initial V = 0
  - Ion starts the gyromotion.

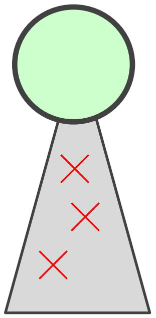

- Photoionization rate
  - $I = 5.1 \times 10^{-9}\ s^{-1}$ [e.g., *Moses and Bass*, 2000]

Ion counts: Comparison with INMS

- Calculated ion counts: INMS: ≈10, Model: 100-1000

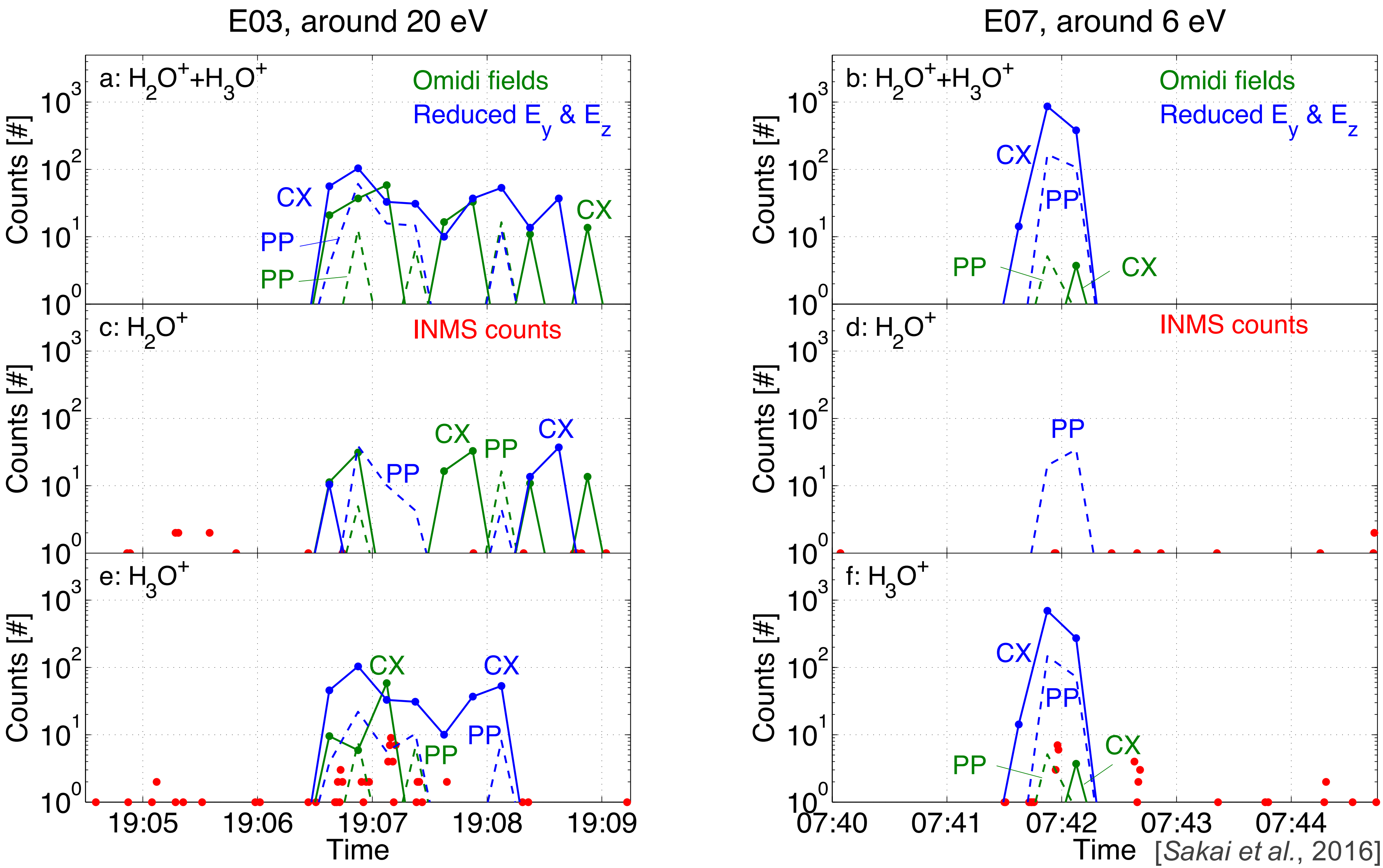

[*Sakai et al.*, 2016]

Model: Flux vs. Counts

- CAPS required the low energy ions in the plume!

	Ion energy (CAPS: E < 10 eV)	**Counts (INMS: ~10)**
Omidi's field	E > 10 eV	10-100
Reduced E	1 eV < E < 10 eV	100-1000

- Why are INMS counts lower than model counts in reduced E?

INMS vs. Model

- Why are INMS counts lower than model?
  - Pointing direction of INMS is important.
    - A slightly shift of the INMS phase-space volume would reduce the model counts.

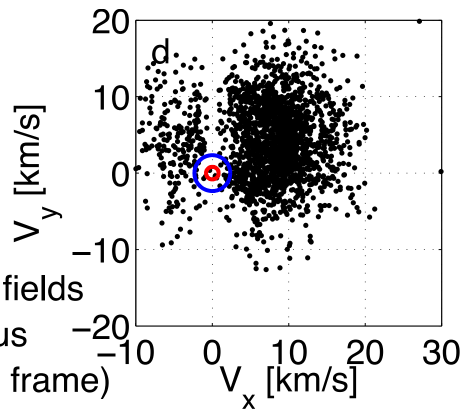

Reduced fields (Enceladus reference frame)

E03

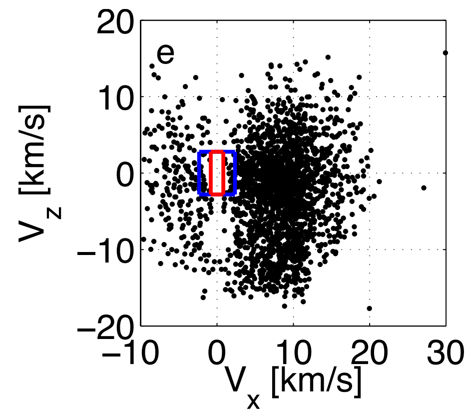

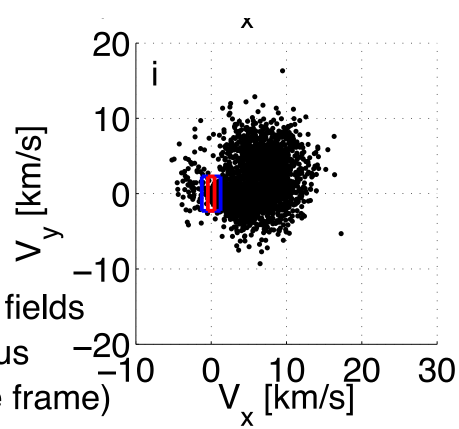

Reduced fields (Enceladus reference frame)

E07

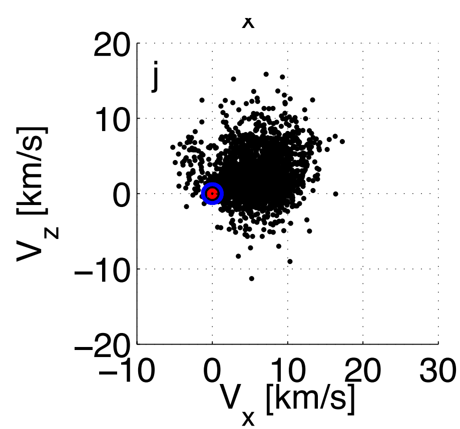

[*Sakai et al.*, 2016]

Ion density in the plume

- Ion density: 400-800 cm^{-3}
  - Langmuir Probe: ~10^4 cm^{-3} [*Morooka et al.*, 2011]
  - Previous model: 100-1000 cm^{-3} [*Kriegel et al.*, 2014]
  - E_y is still low?

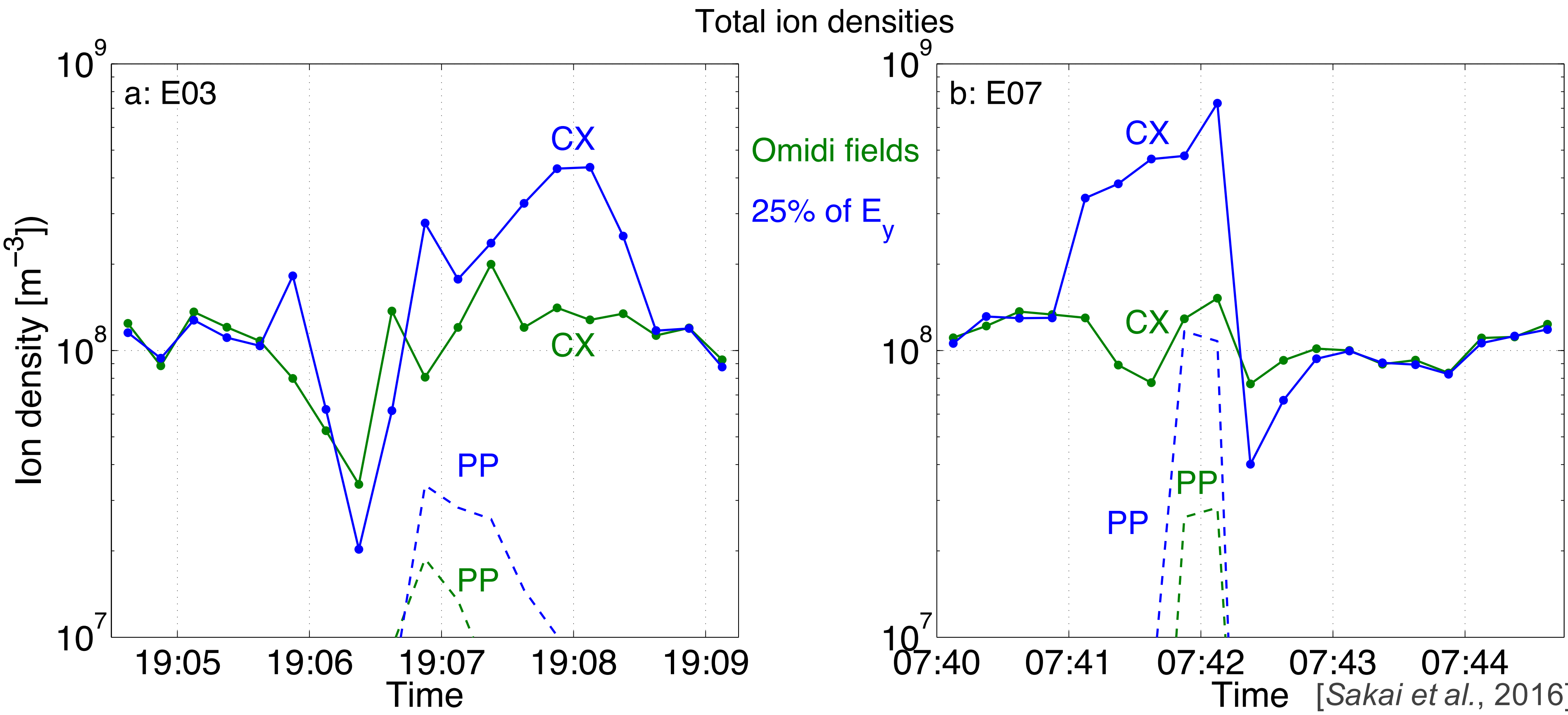

[*Sakai et al.*, 2016]

More reduced E field

- Energy-Flux distribution: 25% vs. 10% of Omidi's E_y
- 10% of Omidi's E_y
  - Consistent with a velocity of ~1 km/s [*Kriegel et al.*, 2011]
- Fluxes did not have big changes in both cases.
  - Ions somewhat get stuck upstream.

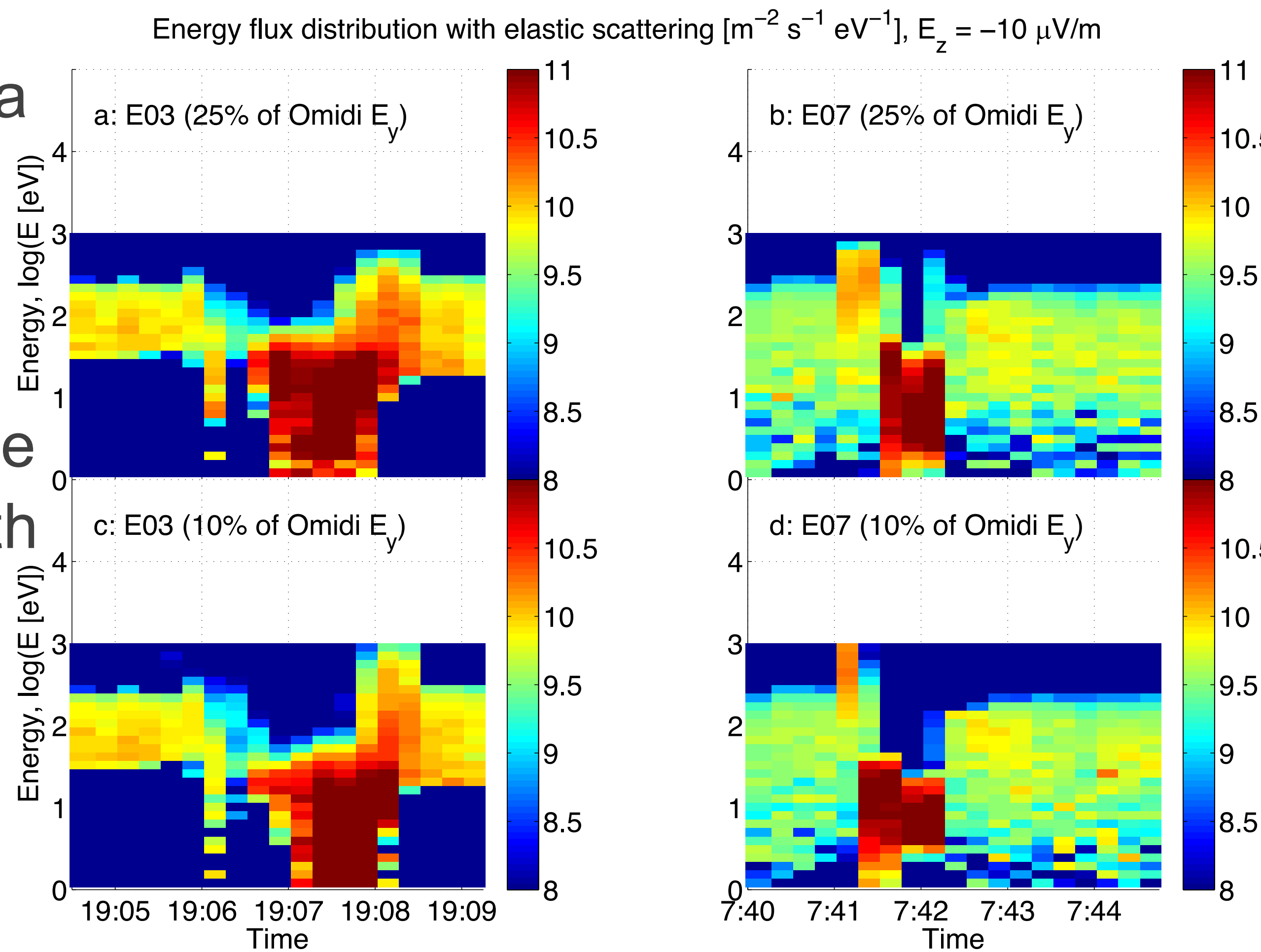

[*Sakai et al.*, 2016]

Ion density

- Ion density: 500-1000 cm^{-3}
  - Langmuir Probe: ~10^4 cm^{-3} [*Morooka et al.*, 2011]
  - Still lower than LP
    - Other effect?: Critical ionization velocity effect [*Meier et al.*, 2015]
  - Note that model ion count with 10% of E_y is almost similar to 25% of E_y.

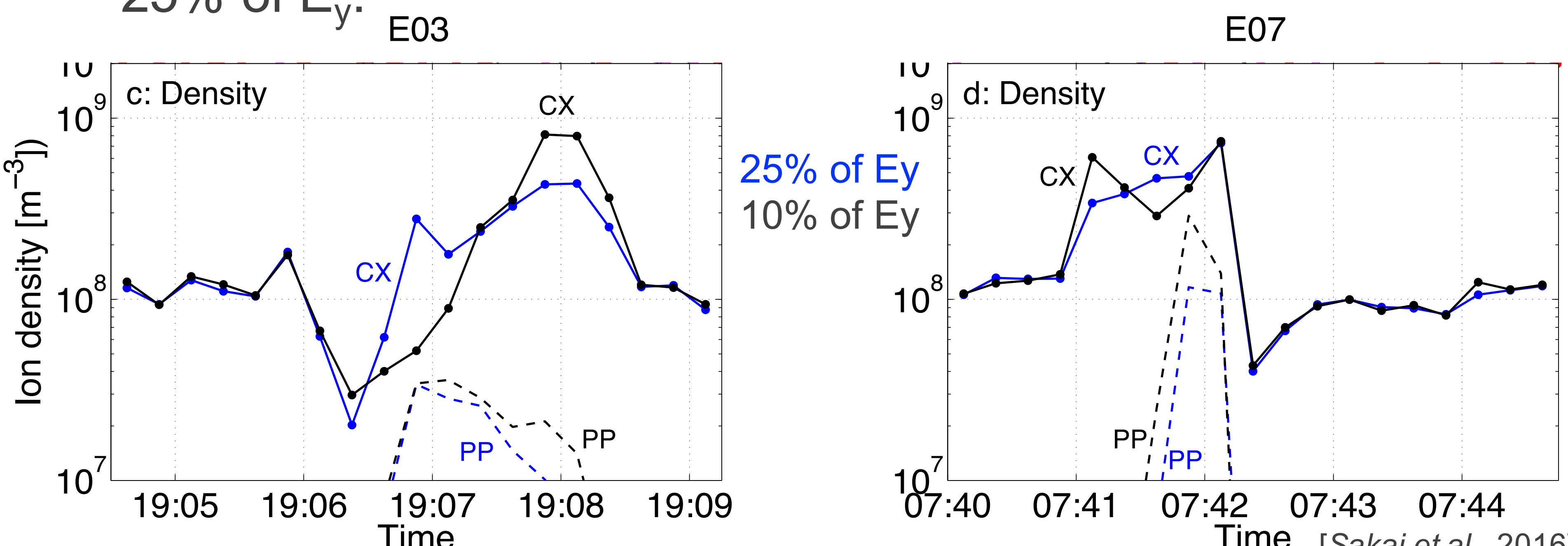

[*Sakai et al.*, 2016]

Summary

THE UNIVERSITY OF KANSAS

- Energy vs. flux distribution
  - Vertical electric field is important for obtaining the low energy ion detected by CAPS.
  - The electric field could be generated by dust or pressure gradient of plasma in Z direction.
- Ion species
  - H_3O^+ is dominant which is consistent with INMS.
  - Our total count is not consistent with INMS results.
    - Direction where INMS is looking significantly affects it.
- Ion density
  - 400-1000 cm^{-3} from our model
  - It is lower than LP even if more reduced E is considered, but almost consistent with previous models.

References

- Cravens, T. E. et al. (2009), Plume iononsphere of Enceladus as seen by the Cassini ion and neutral mass spectrometer, *Geophys. Res. Lett.*, *36*, L08106.
- Gurnett, D. A. et al. (2004), The Cassini Radio and Plasma Wave Investigation, *Space Sci. Rev.*, *114*, 395-463.
- Farrell, W. M. et al. (2010), Modification of plasma in the near-vicinity of Enceladus by the enveloping dust, *Geophys. Res. Lett.*, *37*, L20202.
- Fleshman, B. L. et al. (2010), Modeling the Enceladus plume-plasma interaction, *Geophys. Res. Lett.*, *37*, L03202.
- Holmberg, M. K. G. et al. (2012), Ion densities and velocities in the inner plasma torus of Saturn, *Planet. Space Sci.*, *73*, 151-160.
- Kriegel, H. et al. (2014), Ion densities and magnetic signatures of dust pickup at Enceladus, *J. Geophys. Res. Space Physics*, *119*, 2740-2774.
- Kristic, P. S. and D. R. Schultz (1999), Elastic scattering and charge transfer in slow collisions: isotopes of H and H^+ colliding with isotopes of H and with He, *J. Phys. B*, *32*, 3487-3509.
- Lishawa, C. R. et al. (1990), Cross sections and product kinetic energy analysis of H_2O^+-H_2O collisions at suprathermal energies, *J. Chem. Phys*, *93*, 3196-3206.
- Meier, P. et al. (2015), Modeling the total dust production of Enceladus from stochastic charge equilibrium and simulations, *Planet. Space Sci.*, *119*, 208-221.

References

- Morooka, M. W. et al. (2011), Dusty plasma in the vicinity of Enceladus, *J. Geophys. Res.*, *116*, A12221.
- Moses, J. I., and S. F. Bass (2000), The effects of external material on the chemistry and structure of Saturn's ionosphere, *J. Geophys. Res.*, *105*, 7013-7052.
- Omidi, N. et al. (2012), Flow stagnation at Enceladus: The effects of neutral gas and charged dust, *J. Geophys. Res.*, *117*, A06230.
- Sakai, S. et al. (2013), Dust-plasma interaction through magnetosphere-ionosphere coupling in Saturn's plasma disk, *Planet. Space Sci.*, *75*, 11-18.
- Sakai, S. et al. (2016), Ion energy distributions and densities in the plume of Enceladus, *Planet. Space Sci.*, in press.
- Saur, J. et al. (2008), Evidence for temporal variability of Enceladus' gas jets: Modeling of Cassini observations, *Geophys. Res. Lett.*, *35*, L20105.
- Waite, J. H. Jr. et al. (2004), The Cassini Ion and Neutral Mass Spectrometer (INMS) investigation, *Space Sci. Rev.*, *114*, 113-231.